OPEN ACCESS
JOURNAL OF ADVANCED DIELECTRICS
Vol. 12, No. 6 (2022) 2241003 (6 pages)

DOI: 10.1142/S2010135X2241003X

Effect of Li_2CO_3 addition on structural and electrical properties of $0.7BiFeO_3$-$0.3BaTiO_3$ piezoelectric ceramic

Hongbo Liu* and Jianguo Chen†,‡

*School of Materials Science and Engineering, Shanghai University of Engineering Science
Shanghai 201620, P. R. China

†School of Materials Science and Engineering, Shanghai University
Shanghai 200444, P. R. China

‡kpfocus@shu.edu.cn

Received 18 August 2022; Revised 4 September 2022; Accepted 8 September 2022; Published 19 October 2022

In this work, Li_2CO_3 was added into $0.7BiFeO_3$-$0.3BaZr_{0.02}Ti_{0.98}O_3$-0.01mol$MnO_2$ (70BFBTMn) piezoelectric ceramics to reduce their sintering temperatures. 70BFBTMn ceramics were sintered by a conventional solid reaction method, and their structural, dielectric, piezoelectric and ferroelectric properties were studied. These results indicate that 0.5% (mole) Li_2CO_3 is the optimized content and it can reduce the sintering temperature by 100°C, making the possibility of the piezoelectric ceramics cofiring with Ag electrodes at low temperatures to manufacture multilayer piezoelectric actuators.

Keywords: Piezoelectric ceramics; $BiFeO_3$-$BaTiO_3$; low temperature co-fired ceramic technology.

1. Introduction

High-performance piezoelectric ceramics can be applied in many fields, such as sensors and actuators due to the efficient conversion between mechanical energy and electrical energy. Pb(Zr,Ti)O_3-based ceramics are dominant commercial materials. Currently, because of the toxic Pb element and low depoling temperature (<200°C), Pb-free piezoelectric ceramics are extensively studied for replacing Pb(Zr,Ti)O_3-based ceramics and applying at high temperatures, for instance, bismuth-based,[1] sodium bismuth titanate-based,[2] barium titanate-based,[3,4] potassium sodium niobate-based,[5] etc. Although the market for piezoelectric devices is dominated by Pb(Zr_xTi_{1-x})O_3 ceramics, lead-free piezoelectric ceramics will experience a strong growth.[6,7]

Among them, $BiFeO_3$-$BaTiO_3$ solid solution is regarded as a new generation of lead-free materials.[8] From pure $BaTiO_3$ to pure $BiFeO_3$, the structure of $BiFeO_3$-$BaTiO_3$ varies from tetragonal, pseudocubic, and rhombohedral. The compositions of $BiFeO_3$-$BaTiO_3$ close to a mixed phase region of rhombohedral and pseudocubic have attracted great attention due to excellent piezoelectric properties. Large macrostrain was attributed to lattice distortion, domain switching, and phase transition.[9] It is also reported that high electrostrain is related to the formation of an active pseudosymmetric structure.[10] Ceramics with a rhombohedral phase show much better thermal stability and aging properties than those with mixed pseudocubic and rhombohedral phases.[11] Fast cooling can create core-shell microstructured $BiFeO_3$-$BaTiO_3$ with improved piezoelectric properties,[12] and the detailed nanoscale structural analysis shows the core-shell includes a pseudocubic shell enriched in Ba and Ti, an octahedrally tilted outer core richest in Bi and Fe, and an apparently pseudocubic inner-core phase richer in Ba and very low in Ti.[13] When the content of $BiFeO_3$ is higher than 67%, the solid solution is the rhombohedral phase with the curie temperature higher than 500°C,[11] which makes $BiFeO_3$-$BaTiO_3$ based piezoelectric devices can operate at high temperatures. For instance, after Mn doping the Curie temperature, dielectric constant, dielectric loss, piezoelectric coefficient, and remnant polarization of $0.69BiFeO_3$-$0.31BaTiO_3$ are 598°C, 704, 0.067, 82 pC/N, and 18.8 $\mu C/cm^2$, respectively.[14] In addition, since there is no other phase transition below the Curie temperature, the piezoelectric properties of $BiFeO_3$-$BaTiO_3$ solid solutions are stable at high temperatures. For instance, the piezoelectric coefficient is stable prior to 500°C after air-annealing for Mn-modified $0.75BiFeO_3$-$0.25BaTiO_3$,[15] indicating excellent thermal stability of piezoelectricity and comparable to that of bismuth titanate-based high-temperature piezoceramics.[16]

In the field of high-temperature piezoelectric actuators, low-temperature co-fired ceramic technology is commonly used to obtain large displacement at low voltage. For instance, the $BiFeO_3$-$BaTiO_3$-based multilayer actuator was fabricated using Pt as internal electrodes.[17] Nevertheless, Pt is too expensive to be widely used in industry. The less expensive electrode like Ag is not suitable because the sintering temperatures of $BiFeO_3$-$BaTiO_3$ piezoelectric ceramics

‡Corresponding author.

are commonly higher than 1000°C[11] which is too high for Ag paste used in low-temperature co-fired ceramic technology. Thus, reducing the sintering temperature of $BiFeO_3$-$BaTiO_3$-based ceramics is greatly expected for commercialized applications of $BiFeO_3$-$BaTiO_3$-based ceramics for multilayer actuators. By adding some oxide, the sintering temperature of ceramics can be reduced. For instance, by adding CuO, the sintering temperature of $BiScO_3$-$PbTiO_3$ piezoceramics is reduced and a multilayer actuator with Ag electrodes was successfully fabricated.[18] Thus, it is possible to reduce the sintering temperature of $BiFeO_3$-$BaTiO_3$ by choosing the right sintering assistant oxide. In addition, Bi volatilization during sintering can be inhibited also by reducing the sintering temperature. Since Li_2CO_3 has been proved to be an effective additive to reduce the sintering temperature of piezoceramics,[19–23] in this work, Li_2CO_3 was added in 70BFBTMn to reduce the sintering temperature. In the composition, 1% (mole) Mn was added to improve resistivity,[14,24–26] while 2% (mole) Zr was doped to enhance strain according to our previous works.[27,28]

2. Experimental Procedure

70BFBTMn - xLi_2CO_3 (x = 0.005, 0.01, 0.02, 0.03) ceramics were prepared by a conventional solid-state reaction method. The raw materials used were $BaCO_3$, ZrO_2, Fe_2O_3,

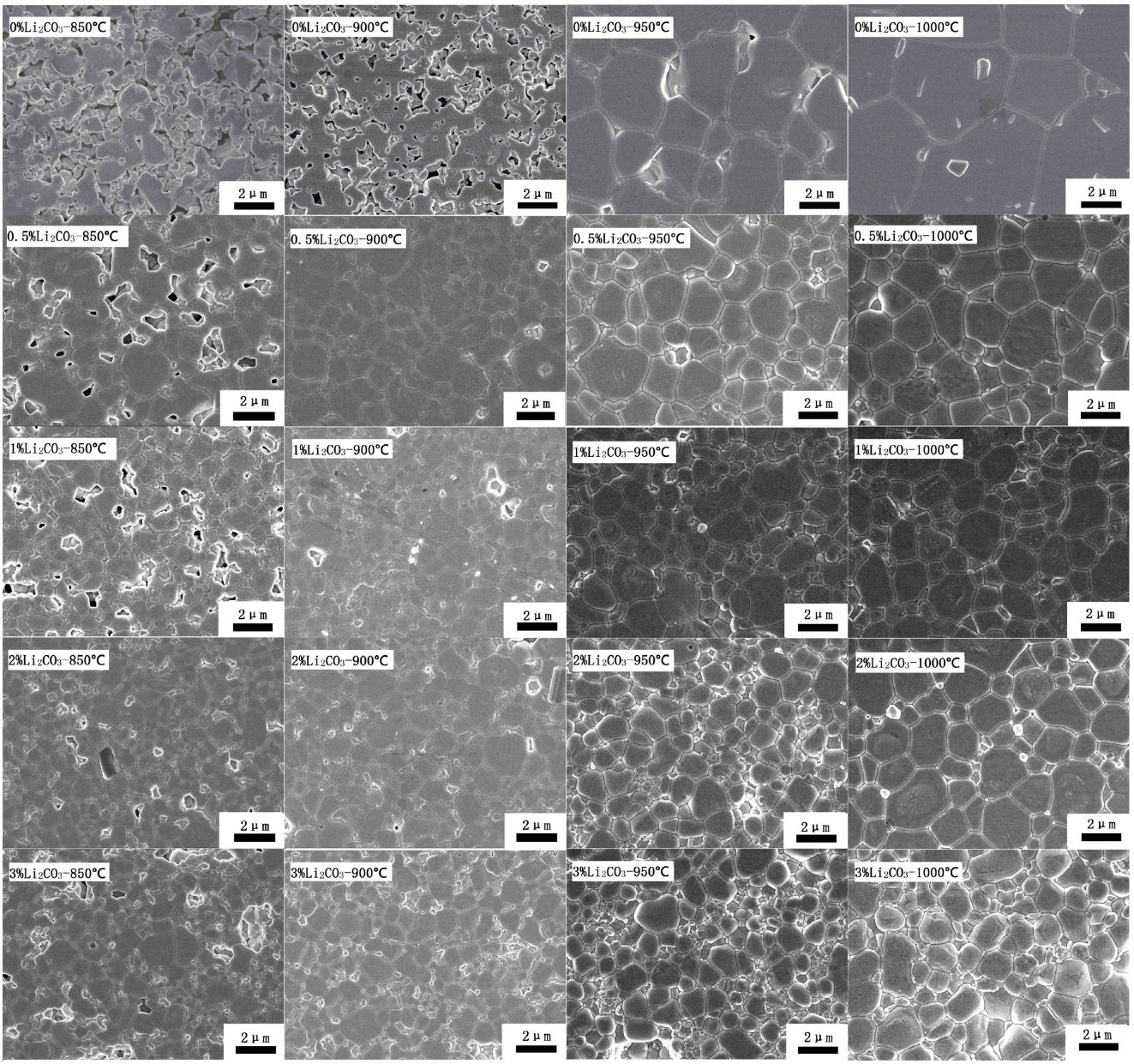

Fig. 1. Microstructures of 70BFBTMn ceramics with different Li_2CO_3 contents sintered at 850°C and 1000°C.

MnO_2, TiO_2, Bi_2O_3, and Li_2CO_3. During the mixing process, 1 mol.% excess Bi was added to compensate for the volatilization of Bi. The raw materials were weighted according to the stoichiometric ratio and ball-milled for 24 h on a planetary ball mill, then the dry powders were calcined at 750°C for 4 h. Then, powders were pressed into pellets of 12 mm in diameter and 1 mm in thickness at a pressure of 150 MPa. The polyvinyl alcohol binder was burned out at 6°C for 4 h. Ceramics were sintered at 850–1000°C for 2 h.

The relative density of ceramic samples was measured by the Archimedes method. The morphology of thermal-etched ceramics was observed by field emission scanning electron microscopy (SEM, Zeiss G300). Phase structures of ceramics were analyzed by X-ray diffraction (XRD, Rigaku-D/MAX-2550) with Cu K_{a1} radiation (λ = 1.54056 Å). The dielectric properties were measured by an Agilent impedance analyzer (Agilent 4294A). Ferroelectric hysteresis loops (P-E) and electric-field-induced strain loops (S-E) of samples were measured by the ferroelectric testing system (TF1000 analyzer) at room temperature.

3. Results and Discussion

The microstructure of 70BFBTMn - xLi_2CO_3 ceramics sintered at different temperatures is shown in Fig. 1. Too many pores were observed in the 70BFBTMn ceramics sintered at 850°C and 900°C without adding Li_2CO_3, and the dense microstructure can be obtained at 1000°C. After adding Li_2CO_3, the pores decrease significantly after 900°C sintering, 950°C sintered ceramics have fine grains and clear grain boundaries, and the size of grains increases for 1000°C sintered ceramics. When the content of Li_2CO_3 is larger than 2%, the shape of grains becomes irregular. These results indicate that the sintering temperature of $0.7BiFeO_3$-$0.3BaZr_{0.02}Ti_{0.98}O_3$ is decreased after adding Li_2CO_3, and the optimized content of Li_2CO_3 is less than 2%. The main reason for lowering the sintering temperature here is transient liquid phase assisted sintering as in the low-temperature synthesis of AlN [29] and Pb-based piezoeletrics[30,31] because the melting temperature Li_2CO_3 is 723°C.[29]

The relative density of 70BFBTMn ceramics with different Li_2CO_3 contents is shown in Fig. 2. The ceramics sintered at 900–1000°C have high densities, and the relative density is above 94% for 70BFBTMn ceramics with Li_2CO_3 addition. For all sintered ceramics, the highest density is 96.4%, which corresponds to 0.5% Li_2CO_3 added 70BFBTMn ceramic sintered at 950°C. Overall, above 900°C is the suitable sintering temperature for Li_2CO_3 modified 70BFBTMn ceramics. Although the complete measurements were done for all sintered ceramics, the effect of doping content is dominant. The following discussions will only focus on the results of 900°C sintered ceramics.

Figure 3 shows the X-ray diffraction patterns of 70BFBTMn ceramics with different Li_2CO_3 contents sintered at 900°C. All the sintered ceramics exhibit pure perovskite

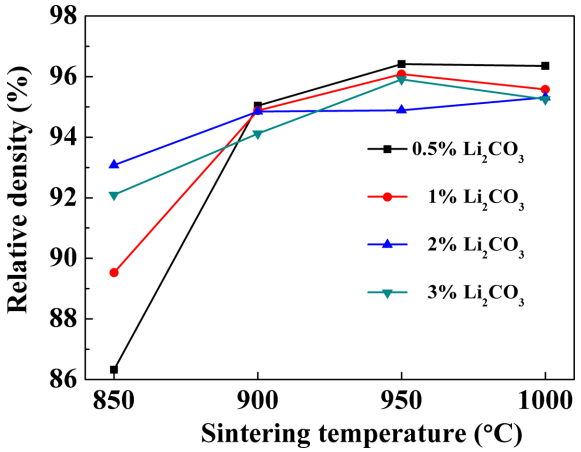

Fig. 2. The relative densities of 70BFBTMn ceramics with different Li_2CO_3 contents sintered at 850°C and 1000°C.

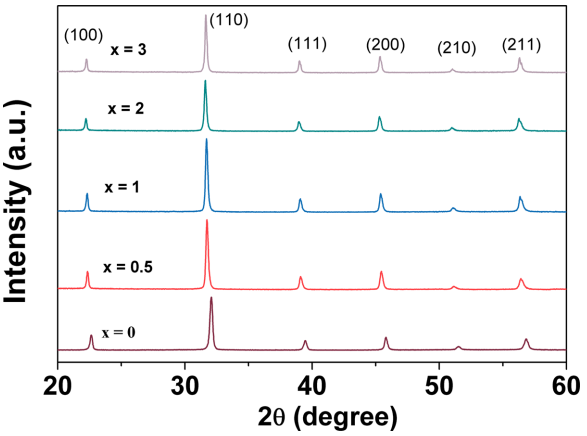

Fig. 3. X-ray diffraction patterns of 70BFBTMn - xLi_2CO_3 ceramics at 900°C.

structure and no impurity phases are observed within the detection limit of X-ray diffraction. Although when the content of $BiFeO_3$ is higher than 67% the rhombohedral structure is expected, neither pseudocubic $(111)_c$ peak nor $(200)_c$ peak splits as shown in Fig. 1, indicating the prepared ceramics are pseudocubic, which could be due to extremely small rhombohedral distortion as reported[14] or more complex core–shell structure.[13]

Dielectric properties of 70BFBTMn - xLi_2CO_3 ceramics are given in Fig. 4. At room temperature for all Li_2CO_3 added ceramics, 0.5% Li_2CO_3 added ceramic has the highest dielectric permittivity from 10^3 Hz to 10^6 Hz as shown in Fig. 4(a). Since at room temperature, the ceramic without Li_2CO_3 has a dielectric permittivity of 632 (1 kHz) and a dielectric loss of 0.045 (1 kHz), the values are 577 and 0.046 for 0.5% Li_2CO added ceramic, suggesting that the dielectric permittivity does not deteriorate significantly and the dielectric loss remains small after adding 0.5% Li_2CO_3. From room temperature to 600°C for all Li_2CO_3 added ceramics, the dielectric loss of 0.5% Li_2CO added ceramic is the lowest as shown in

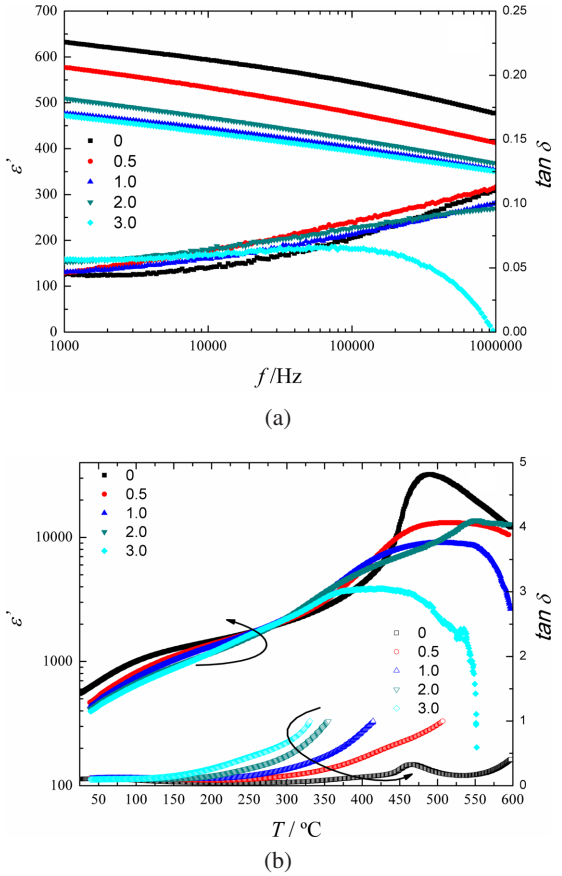

Fig. 4. Frequency-dependent dielectric permittivity and dielectric loss (a), and temperature-dependent dielectric permittivity and dielectric loss (b) of 70BFBTMn - $x$$Li_2CO_3$ ceramics sintered at 900°C.

Fig. 4(b), and the dielectric permittivity of 0.5% Li_2CO added ceramic is like to that of 70BFBTMn. These results indicate that 0.5% Li_2CO adding has the weakest influence on the high-temperature dielectric of all Li_2CO added 70BFBTMn piezoelectric ceramics. For all Li_2CO_3 added ceramics, with increasing temperature dielectric loss increases significantly. This could be related to Li replacing the A-site or B-site of the perovskite structure creating more oxygen vacancies. The mobility of oxygen vacancies increases at high temperatures, thus the conductivity of the ceramics increases. As a result, the dielectric loss rises at high temperatures.

Figure 5 shows ferroelectric hysteresis loops, bipolar, and unipolar strains of 70BFBTMn - $x$$Li_2CO_3$ ceramics at room temperature. All ceramics show typical ferroelectric hysteresis loops as shown in Fig. 5(a). At an applied electric field of 80 kV/cm (1 Hz), the polarization is 32.0 μC/cm^2, 27.7 μC/cm^2, 16.8 μC/cm^2, 14.8 μC/cm^2, and 13.0 μC/cm^2, the remanent polarization is 22.3 μC/cm^2, 16.2 μC/cm^2, 9.8 μC/cm^2, 7.6 μC/cm^2, 6.6 μC/cm^2, and the coercive field is 40 kV/cm, 33 kV/cm, 37 kV/cm, 30 kV/cm, and 33 kV/cm, for x = 0, 0.5, 1, 2, and 3, respectively.

The bipolar and unipolar strain hysteresis loops of 70BFBTMn - $x$$Li_2CO_3$ ceramics are shown in Figs. 5(b) and

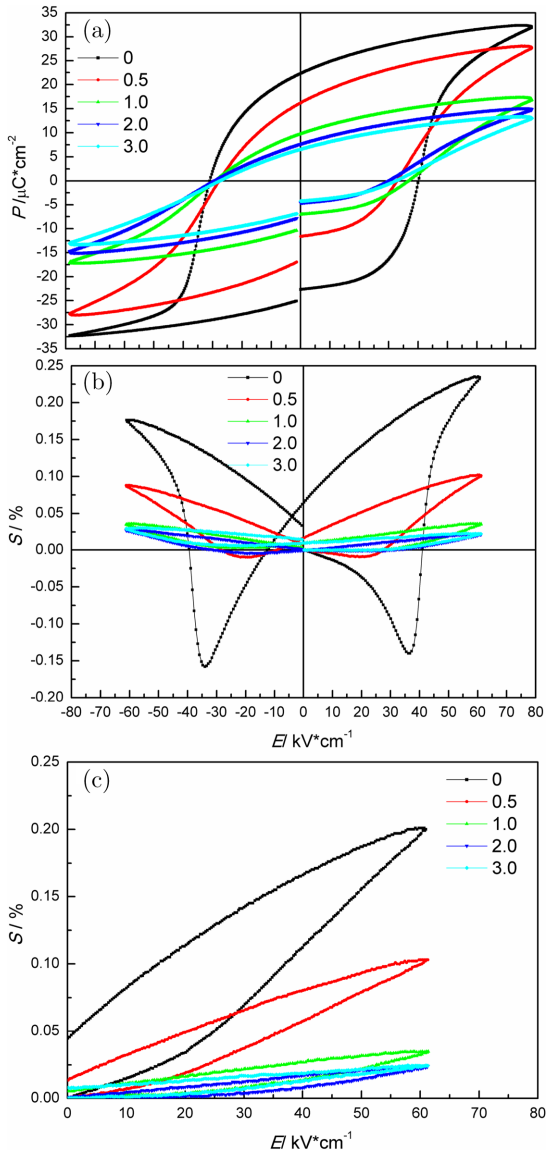

Fig. 5. Ferroelectric hysteresis loops (a), bipolar strain loops (b), and unipolar strain loops (c) of 70BFBTMn - $x$$Li_2CO_3$ ceramics sintered at 900°C.

5(c). The standard butterfly curves are observed for all ceramics. The bipolar strain of 70BFBTMn is 0.235%. The bipolar strain of 0.5% Li_2CO_3 added ceramic reaches up to 0.102%, much higher than other Li_2CO_3 added ceramics (varying from 0.021 to 0.036). The unipolar strain curves are shown in Fig. 5(c). The stain at 60 kV/cm is 0.200%, 0.103%, 0.035%, 0.024%, and 0.024 for x = 0, 0.5, 1, 2, and 3, respectively. The high field strain coefficient d^*_{33} was calculated by $d^*_{33}=S_{max}/E_{max}$, where S_{max} is the largest strain, and E_{max} is the highest applied electric field. d^*_{33} is 333 pm/V, 171 pm/V, 58 pm/V, 40 pm/V, and 40 pm/V for x = 0, 0.5, 1, 2, and 3, respectively.

Above electrical properties indicate that the ferroelectric, piezoelectric, and dielectric properties of 70BFBTMn deteriorate after adding Li_2CO_3, which could be related to the

reduced size of grains as shown in Fig. 1, grain boundaries with Lirich, and Li partly replacing A-site or B-site of the perovskite structure.

4. Conclusion

$0.7Bi_{0.5}FeO_3$-$0.3BaZr_{0.02}Ti_{0.98}O_3$-$0.01MnO_2$-$xLi_2CO_3$ (x = 0.5%, 1%, 2%, 3%) piezoelectric ceramics were prepared by the conventional solid reaction method with varying the sintering temperature from 850°C to 1000°C. Dense ceramics are obtained when the sintering temperature is higher than 900°C. Thus, Li_2CO_3 doping can effectively reduce the sintering temperature of $0.7Bi_{0.5}FeO_3$-$0.3BaZr_{0.02}Ti_{0.98}O_3$-$0.01MnO_2$ from 1000°C to 900°C. For 900°C sintered ceramics, pure perovskite structure can be obtained when varying the content of Li_2CO_3 from 0.5% to 3%. 0.5% Li_2CO_3 added ceramic deteriorates the electrical properties of $0.7Bi_{0.5}FeO_3$-$0.3BaZr_{0.02}Ti_{0.98}O_3$-$0.01MnO_2$ slightly with a dielectric permittivity of 577 (1 kHz), a dielectric loss of 0.046 (1 kHz), a of 27.7 $\mu C/cm^2$, a strain of 0.102%, and a high field strain coefficient d^*_{33} of 171 pm/V. Thus, 0.5% Li_2CO_3 added $0.7Bi_{0.5}FeO_3$-$0.3BaZr_{0.02}Ti_{0.98}O_3$-$0.01MnO_2$ piezoelectric ceramic is expected to co-fire with Ag paste to prepare multilayer actuators using low temperature co-fired ceramic technology.

Acknowledgments

The work was supported by the National Natural Science Foundation of China (Grant Nos. 11704242, 51872180 and 51672169) and the Natural Science Foundation of Shanghai, China (Grant Nos. 17ZR1447200 and 18ZR1414800).

References

[1]Z. Liu, H. Wu, Y. Yuan, H. Wan, Z. Luo, P. Gao, J. Zhuang, J. Zhang, N. Zhang, J. Li, Y. Zhan, W. Ren and Z.-G. Ye, Recent progress in bismuth-based high Curie temperature piezo-/ferroelectric perovskites for electromechanical transduction applications, *Curr. Opin. Solid State Mater. Sci.* **26**(5), 101016 (2022).

[2]J. Hao, W. Li, J. Zhai and H. Chen, Progress in high-strain perovskite piezoelectric ceramics, *Mater. Sci. Eng. R Rep.* **135**, 1 (2019).

[3]P. K. Panda, B. Sahoo, T. S. Thejas and M. Krishna, High d33 Lead-free piezoceramics: A review, *J. Electron. Mater.* **51**(3), 938 (2022).

[4]M. Acosta, N. Novak, V. Rojas, S. Patel, R. Vaish, J. Koruza, G. A. Rossetti and J. Rödel, $BaTiO_3$-based piezoelectrics: Fundamentals, current status, and perspectives, *Appl. Phys. Rev.* **4**(4), 041305 (2017).

[5]H. Liu, Y.-X. Liu, A. Song, Q. Li, Y. Yin, F.-Z. Yao, K. Wang, W. Gong, B.-P. Zhang and J.-F. Li, (K, Na)NbO_3-based lead-free piezoceramics: One more step to boost applications, *Natl. Sci. Rev.* **9**(8), nwac101 (2022).

[6]W. Jo, R. Dittmer, M. Acosta, J. Zang, C. Groh, E. Sapper, K. Wang and J. Rödel, Giant electric-field-induced strains in lead-free ceramics for actuator applications – status and perspective, *J. Electroceramics* **29**(1), 71 (2012).

[7]J. Rödel and J.-F. Li, Lead-free piezoceramics: Status and perspectives, *MRS Bull.* 576 (2018).

[8]D. Wang, G. Wang, S. Murakami, Z. Fan, A. Feteira, D. Zhou, S. Sun, Q. Zhao and I. M. Reaney, $BiFeO_3$-$BaTiO_3$: A new generation of lead-free electroceramics, *J. Adv. Dielectr.* **8**(6), 1830004 (2018).

[9]J. Chen, J. E. Daniels, J. Jian, Z. Cheng, J. Cheng, J. Wang, Q. Gu and S. Zhang, Origin of large electric-field-induced strain in pseudo-cubic $BiFeO_3$–$BaTiO_3$ ceramics, *Acta Mater.* **197**, 1 (2020).

[10]G. Wang, Z. Fan, S. Murakami, Z. Lu, D. A. Hall, D. C. Sinclair, A. Feteira, X. Tan, J. L. Jones, A. K. Kleppe, D. Wang and I. M. Reaney, Origin of the large electrostrain in $BiFeO_3$-$BaTiO_3$ based lead-free ceramics, *J. Mater. Chem. A* **7**(37), 21254 (2019).

[11]J. Chen, J. Cheng, J. Guo, Z. Cheng, J. Wang, H. Liu and S. Zhang, Excellent thermal stability and aging behaviors in $BiFeO_3$-$BaTiO_3$ piezoelectric ceramics with rhombohedral phase, *J. Am. Ceram. Soc.* **103**(1), 374 (2020).

[12]I. Calisir, A. K. Kleppe, A. Feteira and D. A. Hall, Quenching-assisted actuation mechanisms in core–shell structured $BiFeO_3$–$BaTiO_3$ piezoceramics, *J. Mater. Chem. C* **7**(33), 10218 (2019).

[13]S. J. McCartan, I. Calisir, G. W. Paterson, R. W. H. Webster, T. A. Macgregor, D. A. Hall and I. MacLaren, Correlative chemical and structural nanocharacterization of a pseudo-binary $0.75Bi(Fe_{0.97}Ti_{0.03})O_3$-$0.25BaTiO_3$ ceramic, *J. Am. Ceram. Soc.* **104**(5), 2388 (2021).

[14]S. O. Leontsev and R. E. Eitel, Dielectric and Piezoelectric Properties in Mn-Modified $(1-x)BiFeO_3$–$xBaTiO_3$ Ceramics, *J. Am. Ceram. Soc.* **92**(12), 2957 (2009).

[15]J. Chen, B. Tong, J. Lin, X. Gao, J. Cheng and S. Zhang, Tailoring the chemical heterogeneity of Mn-modified $0.75BiFeO_3$-$0.25BaTiO_3$ ceramics for piezoelectric sensor applications, *J. Eur. Ceram. Soc.* **42**(9), 3857 (2022).

[16]X. Xie, Z. Zhou, R. Liang and X. Dong, Superior piezoelectricity in bismuth titanate-based lead-free high-temperature piezoceramics via domain engineering, *Adv. Electron. Mater.* **8**(7), 2101266 (2022).

[17]S. Murakami, D. Wang, A. Mostaed, A. Khesro, A. Feteira, D. C. Sinclair, Z. Fan, X. Tan and I. M. Reaney, High strain (0.4%) $Bi(Mg_{2/3}Nb_{1/3})O_3$-$BaTiO_3$-$BiFeO_3$ lead-free piezoelectric ceramics and multilayers, *J. Am. Ceram. Soc.* **101**(12), 5428 (2018).

[18]M. A. Qaiser, X.-Z. Ma, R. Ma, W. Ali, X. Xu, G. Yuan and L. Chen, High-temperature multilayer actuators based on CuO added $BiScO_3$–$PbTiO_3$ piezoceramics and Ag electrodes, *J. Am. Ceram. Soc.* **102**(9), 5424 (2019).

[19]G. F. Fan, M. B. Shi, W. Z. Lu, Y. Q. Wang and F. Liang, Effects of Li_2CO_3 and Sm_2O_3 additives on low-temperature sintering and piezoelectric properties of PZN-PZT ceramics, *J. Eur. Ceram. Soc.* **34**(1), 23 (2014).

[20]X.-Y. Tong, J.-J. Zhou, K. Wang, H. Liu and J.-Z. Fang, Low-temperature sintered $Bi_{0.5}Na_{0.5}TiO_3$-$SrTiO_3$ incipient piezoceramics and the co-fired multilayer piezoactuator thereof, *J. Eur. Ceram. Soc.* **37**(15), 4617 (2017).

[21]S. Guan, H. Yang, Y. Zhao and R. Zhang, Effect of Li_2CO_3 addition in $BiFeO_3$-$BaTiO_3$ ceramics on the sintering temperature, electrical properties and phase transition, *J. Alloys Compd.* **735**, 386 (2018).

[22]H. Yuan, L. Li, H. Hong, Z. Ying, X. Zheng, L. Zhang, F. Wen, Z. Xu, W. Wu and G. Wang, Low sintering temperature, large strain and reduced strain hysteresis of $BiFeO_3$–$BaTiO_3$ ceramics for piezoelectric multilayer actuator applications, *Ceram. Int.* **47**(22), 31349 (2021).

[23]S. Guan, H. Yang, G. Qiao, Y. Sun, F. Qin and H. Hou, Effects of Li_2CO_3 and CuO as composite sintering aids on the structure, piezoelectric properties, and temperature stability of $BiFeO_3$-$BaTiO_3$ Ceramics, *J. Electron. Mater.* **49**(10), 6199 (2020).

[24]Y. Ren, H. Liu, F. Liu and G. Liu, Tuning of electric and magnetic properties of $BiFeO_3$-$SrTiO_3$ solid solution ceramics by site-specific doping of Mn, *J. Alloys Compd.* **877**, 160239 (2021).
[25]L. Hai and H. Liu, Effects of Mn doping on electrical properties of $BiFeO_3$–$SrTiO_3$ solid solution, *Solid State Commun.* **343**, 114652 (2022).
[26]H. Liu and Y. Sun, Defect chemistry for Mn-doped and Nb-doped $BiFeO_3$-based ceramics, *J. Phys. Chem. Solids* **170**, 110951 (2022).
[27]J. Chen and J. Cheng, High electric-induced strain and temperature-dependent piezoelectric properties of 0.75BF–0.25BZT lead-free ceramics, *J. Am. Ceram. Soc.* **99**(2), 536 (2016).
[28]D. Fu, Z. Ning, D. Hu, J. Cheng, F. Wang and J. Chen, Large and temperature-insensitive piezoelectric strain in $xBiFeO_3$–(1−x) $Ba(Zr_{0.05}Ti_{0.95})O_3$ lead-free piezoelectric ceramics, *J. Mater. Sci.* **54**(2), 1153 (2019).
[29]Y. Kameshima, M. Irie, A. Yasumori and K. Okada, Low temperature synthesis of AlN by addition of various Li-salts, *J. Eur. Ceram. Soc.* **24**(15), 3801 (2004).
[30]L. Li, N. Zhang, C. Bai, X. Chu and Z. Gui, Multilayer piezoelectric ceramic transformer with low temperature sintering, *J. Mater. Sci.* **41**(1), 155 (2006).
[31]Y.-D. Hou, L.-M. Chang, M.-K. Zhu, X.-M. Song and H. Yan, Effect of Li_2CO_3 addition on the dielectric and piezoelectric responses in the low-temperature sintered 0.5PZN–0.5PZT systems, *J. Appl. Phys.* **102**(8), 084507 (2007).